

Numerical simulation of fluid dynamics and mixing in headers of sodium-air heat exchangers^{*}

Timur R. Smetanin¹, Vasilii V. Pakholkov¹, Sergey A. Rogozhkin¹, Sergey F. Shepelev¹

¹ Afrikantov OKBM JSC, 15 Burnakovskiy pr., 603074 Nizhny Novgorod, Russia

Corresponding author: Timur R. Smetanin (smetanin_tr@okbm.nnov.ru)

Academic editor: Yury Korovin ♦ **Received** 23 December 2023 ♦ **Accepted** 30 January 2024 ♦ **Published** 26 March 2024

Citation: Smetanin TR, Pakholkov VV, Rogozhkin SA, Shepelev SF (2024) Numerical simulation of fluid dynamics and mixing in headers of sodium-air heat exchangers. Nuclear Energy and Technology 10(1): 27–32. <https://doi.org/10.3897/nucet.10.122352>

Abstract

The paper presents the results of a numerical simulation for sodium fluid dynamics and mixing in the tubing system of an air-cooled heat exchanger (AHX), which is a part of the emergency cooldown system (ECS) of sodium fast reactors (SFRs). Non-uniform sodium flows in the AHX tubing system may lead to the mixing of different-temperature sodium flows, temperature fluctuations and tube breaks. It was found in the course of investigating accidents involving breaks in the PFR and Phénix reactor AHX tubing systems that the failure was caused by the metal temperature fluctuations (Cruickshank and Judd 2005).

The numerical simulation used three- and one-dimensional computer codes. It has been found that the calculations of the AHX sodium flow rate distribution with a practically acceptable accuracy can be performed using a one-dimensional code. The factors that influence the non-uniform distribution of sodium flows in the AHX tubing system have been analyzed. Calculations have been performed for the AHX sodium flow distributions and for the mixing of different-temperature sodium flows in the AHX outlet header. The results are presented from calculating the amplitude of sodium fluctuations near the AHX header walls. The effect from shutting down several modules on the non-uniform flow distribution and temperature fluctuations in the AHX has been investigated. Approximations of numerical solutions have been obtained for the sodium flow distribution as a function of the number of the modules shut down.

Keywords

BN reactors, AHX, sodium, mixing, CFD, hydrodynamics, unevenness, leaks, pulsations

Introduction

One of the safety systems in BN reactors is the emergency cooldown system (ECS) designed to dissipate into the environment the residual reactor heat in the event of the system power loss, loss of feedwater supply and a seismic impact. The ECS includes an air-cooled heat exchanger (AHX) in which heat is transferred from sodium inside the tubes to the atmospheric air in the shell side.

Non-uniform sodium flow rates in the AHX tubing system may cause mixing of different-temperature sodium flows and temperature fluctuations. High heat conductivity of sodium leads to high coefficients of heat transfer, as compared with water or gas, and minor temperature differences between the coolant and the wall, this causing temperature fluctuations penetrating deep into the wall. Thermocyclic fatigue of the wall material may lead to tube breaks and sodium leakage (Kolesnichenko et al. 2023).

^{*} Russian text published: Izvestiya vuzov. Yadernaya Energetika (ISSN 0204-3327), 2023, n. 4, pp. 49–60.

For instance, there were breaks recorded in 1984 in the PFR reactor's tubing system (Cruickshank and Judd 2005). It was found in the course of the investigation that the failure was the result of the temperature fluctuations caused by the heat-exchange tubes having been 'clogged' with undissolved gas. Similar effects were observed in the process of testing the AHX of the Phénix experimental reactor. Therefore, analyzing the fluid dynamics and mixing of different-temperature flows in the AHX is critical for developers of Russian BN reactors.

AHX description

Fig. 1 shows a scheme of the AHX tubing system. The sodium circulation path in the AHX comprises a tube bundle, a horizontal inlet header and a horizontal outlet header (Kolomiyets et al. 2014). The tube bundle consists of heat-exchange modules connected in parallel. Each module consists of parallel U-shaped heat-exchange tubes with an internal diameter of 18 mm integrated through the module's inlet and outlet headers. A two-pass crossflow principle is used for the AHX heat exchange. The heat-exchange tubes have welded single-pass spiral finning for intensifying heat transfer to air. The coolant circulation pattern is the same as in the PFR, PFBR and Monju reactor AHXs (Mochizuki and Takano 2009).

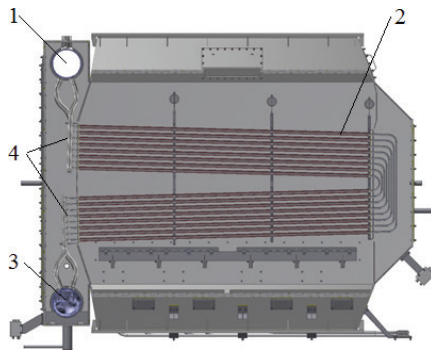


Figure 1. AHX tubing system: 1 – inlet header; 2 – heat-exchange tubes; 3 – outlet header; 4 – module headers.

The heat-exchange tubes in the module have different length and, therefore, different hydraulic resistance. This may lead to a difference in the flow rates in tubes, which may cause undesired temperature fluctuations. In addition, this may also lead to non-uniform distribution of sodium flows by the AHX modules. No effect of undissolved gas on the AHX header fluid dynamics was considered in this study.

The rated AHX parameters in the reactor cooldown mode are presented in Table 1.

Investigation procedure

The AHX was calculated using the CFD FlowVision code and the Piping Systems FluidFlow one-dimensional code (FluidFlow hereinafter) (FluidFlow. User Guide).

Table 1. Rated AHX parameters

Parameter	Value
Thermal power, MW	13
Sodium flow rate, kg/s	52
Sodium temperature, °C:	
– inlet;	505
– outlet	309
Air temperature, °C:	
– inlet;	39
– outlet	307

To simulate the turbulent coolant flow in the AHX flow area, the FlowVision code uses a standard k - ϵ turbulence model complemented with a module of turbulent heat transfer in liquid metal coolant (Liquid Metal Sodium, or LMS) (Aksenov et al. 2014). The FlowVision code was verified with respect to the mixing of different-temperature sodium flows based on experimental data (Knebel et al. 1998; Kimura et al. 2007).

The FluidFlow code allows solving one-dimensional hydraulics equations using reference data on resistances of the hydraulic network's standard components (tube, bend, T-joints) (Idelchik 1992).

The studies were conducted in the following sequence:

- calculation of the sodium flow rate distribution by tubes within one module and in the AHX as the whole;
- estimation of the sodium temperature at the outlet of the module headers;
- analysis of the tube plugging on the mixing in the AHX outlet header.

The geometrical model for calculating the distribution of sodium flow rates by the tubes in the module is presented in Fig. 2a, the model for calculating the distribution of sodium flow rates by the modules in the AHX is presented in Fig. 2b, and the model for estimating the sodium temperature in the outlet header is presented in Fig. 2c.

All heat-exchange tubes in the module header model (see Fig. 2a) are straight and of the same length, and the headers are opposite to each other. There is a lumped hydraulic resistance set on each tube in the model (modifier) that takes into account the local resistance in bends and the friction loss in the tube straight runs. The modifier resistance was calculated based on reference data (Idelchik 1992). Parallelepipeds were used to plot the computational grid in the FlowVision code. The computational grid has mesh clustering in the region of the tube attachment to the headers, the total number of meshes being 258 870.

The AHX model (see Fig. 2b) has the inlet header and the outlet header connected by straight tubes of the same diameter as the module header diameter and the hydraulic resistance of tubes equivalent to the module resistance. This model was used to calculate the non-uniformity of the sodium distribution by modules.

The mixing of different-temperature sodium flows at the module outlet was analyzed on the AHX outlet header model (see Fig. 2c) with an internal diameter of 200 mm. The computational grid has mesh clustering in the outlet

header region and in the wall region, the total number of meshes being 337 620. The value of the parameter y^+ for the module header model and the outlet header model lies in a range of 50 to 100. The sodium flow was simulated on both models as part of the standard $k-\varepsilon$ turbulence model.

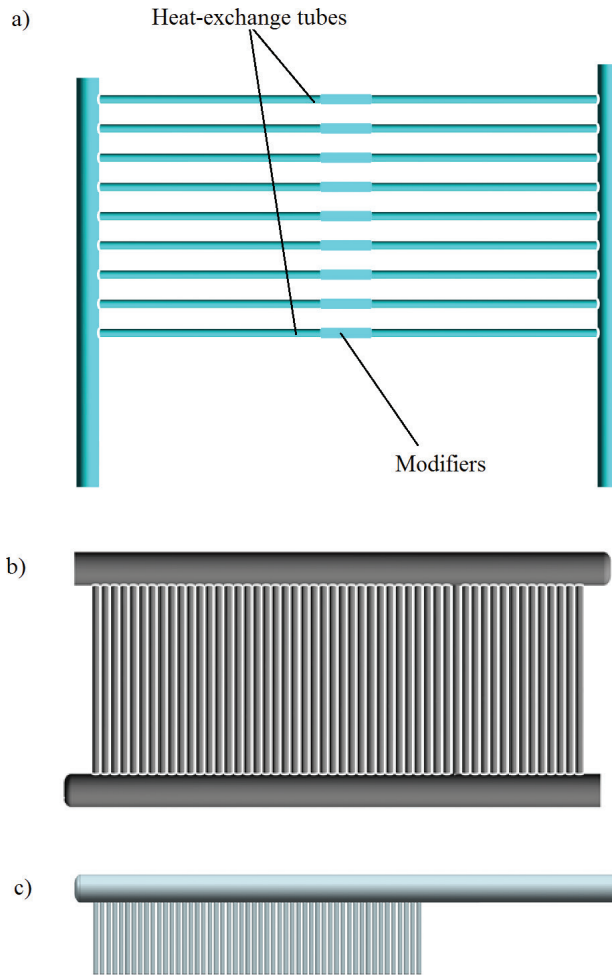


Figure 2. Geometrical models for: a) module headers; b) AHX; c) AHX outlet header

Calculation of the sodium flow rate distribution by the module tubes

The non-uniformity coefficient was taken as the flow rate distribution non-uniformity measure:

$$Z = G_{\max} / G_{\min}, \quad (1)$$

where G_{\max} and G_{\min} are the maximum and the minimum sodium mass flow rates by the module tubes or by the AHX modules, kg/s.

The FlowVision calculations of the sodium flow distribution by the tubes within one module have shown that the non-uniformity coefficient Z is 1.04. The FluidFlow-calculated coefficient Z was 1.10. A comparison of the calculation results obtained using the two codes with the rated AHX parameters (see Table 1) is presented in

Fig. 3 and in Table 2. It follows from Table 2 that some 70% of the total hydraulic loss in the module have been caused by the loss in the tubes.

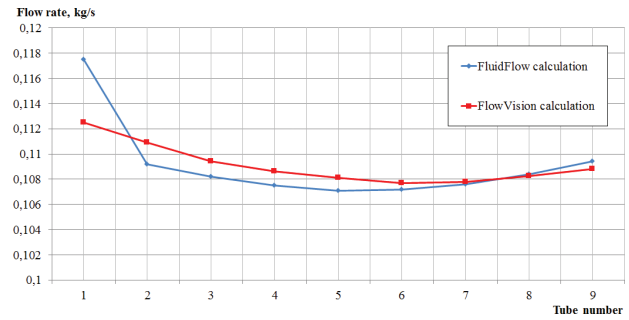


Figure 3. Sodium flow rate distribution by the module tubes.

Table 2. Hydraulic loss in the module

Parameter	Code	
	FlowVision	FluidFlow
Hydraulic loss in heat-transfer tubes, Pa	1138	1371
Hydraulic loss in module headers, Pa	669	431
Total hydraulic loss in module, Pa	1807	1802

Additionally, a number of calculations were undertaken with a flow rate twice as small and 1.2, 1.6 and 2 times as high as the rated value (see Table 1). The maximum non-uniformity of the sodium flow distribution by the module tubes is 1.04 for the FlowVision code and 1.10 for the FluidFlow code.

In the investigated flow rate range, the Reynolds number varies between $4 \cdot 10^4$ and $2 \cdot 10^5$. The flow rate variation does not have effect on the hydraulic resistance coefficient of the module and on the flow rate distribution by the tubes so, accordingly, there is self-similarity of the Reynolds number taking place.

Calculation of the sodium flow rate distribution by the AHX modules

Based on the obtained values of the module resistances, the sodium flow rate distribution by the AHX modules was analyzed using the FlowVision and FluidFlow codes.

As the result of calculating the sodium distribution by the modules, the sodium temperature at the outlet of each module was estimated as a function of the flow rate through the given module:

$$t_{\text{out}} = t_{\text{air}} + (t_{\text{in}} - t_{\text{air}}) e^{-Kndl/(Gc)}, \quad (2)$$

where t_{in} and t_{out} are the module inlet and outlet sodium temperatures, °C; t_{air} is the cooling air temperature, °C; K is the overall heat transfer coefficient, $\text{W}/(\text{m}^2 \cdot \text{°C})$; d is the diameter of the heat-exchange tube, m; l is the tube length, m; G is the sodium flow rate through the tube, kg/s; and c is the sodium heat capacity, $\text{J}/(\text{kg} \cdot \text{°C})$.

With regard for the rated values of the sodium and air temperatures at the AHX inlet and outlet (see Table 1),

the overall heat transfer coefficient was determined. Then, the sodium temperature at the outlet of each module was calculated using formula (2) based on the known sodium flow rate distribution by the AHX modules. The following was assumed for the calculation:

- the air temperature in the AHX is constant throughout the volume;
- no non-uniform air heating in the AHX tube bundle volume with the modules plugged was taken into account.

Fig. 4 presents the calculation results with the header diameter of 200 mm.

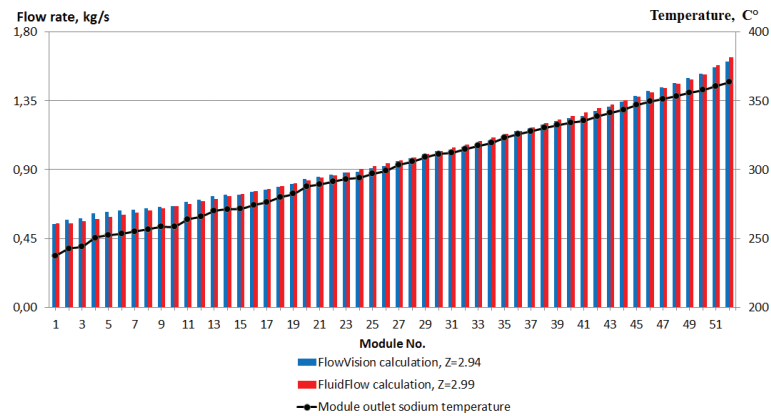


Figure 4. Sodium flow rate distribution by modules and the AHX module outlet temperatures with the header internal diameter of 200 mm.

The non-uniformity coefficient Z for the FlowVision and FluidFlow codes is 2.94 and 2.99 respectively, so the one-dimensional FluidFlow code can be used to calculate the sodium flow rate distribution in the header with the practically acceptable accuracy.

As estimated, the sodium temperature difference at the outlet from the extreme modules with all modules being in operation is 126 °C, and the temperature difference between neighboring modules is in a range of 1 to 6 °C.

The increase in the module outlet sodium temperature in the direction of the sodium flow in the outlet header leads to the formation of large volumes (with the dimensions approximately equal to the collecting header diameter) with conditionally ‘cold’ sodium. The process by which the said volumes are formed and move in the AHX outlet header is shown in Fig. 5 with a time step of 0.4 s. The module includes test points for analyzing the amplitudes of the sodium temperature near the header walls: points 1, 2 and 3 are above module headers 1, 26 and 52 respectively, and point 4 is 7 cm downstream of module header 52.

There are four volumes with ‘cold’ sodium (numbered I through IV in Fig. 5). The evolution of the ‘cold’ sodium volumes in the main flow can be shown clearly by the example of the volumes identified.

None of the considered ‘cold’ sodium volumes have enough time to be heated to the average AHX outlet header temperature. The temperature difference between the main flow and the sodium that comes from the modules is

30 °C in the header middle and increases in the direction of the sodium flow, this leading to temperature fluctuations on the header metal shell.

The maximum amplitude of the sodium temperature fluctuations near the wall (defined as the temperature interval which includes 95% of the calculation points) is reached at test point 3 and amounts to 45 °C.

Near point 3, the difference between the main flow and the sodium that comes from the modules reaches the maximum, so the ‘hot’ sodium vortices at the module outlet create major temperature fluctuations near the header wall at point 3. No such process is observed at points 1 and 4, and a similar process does not lead to major fluctuations at point 2.

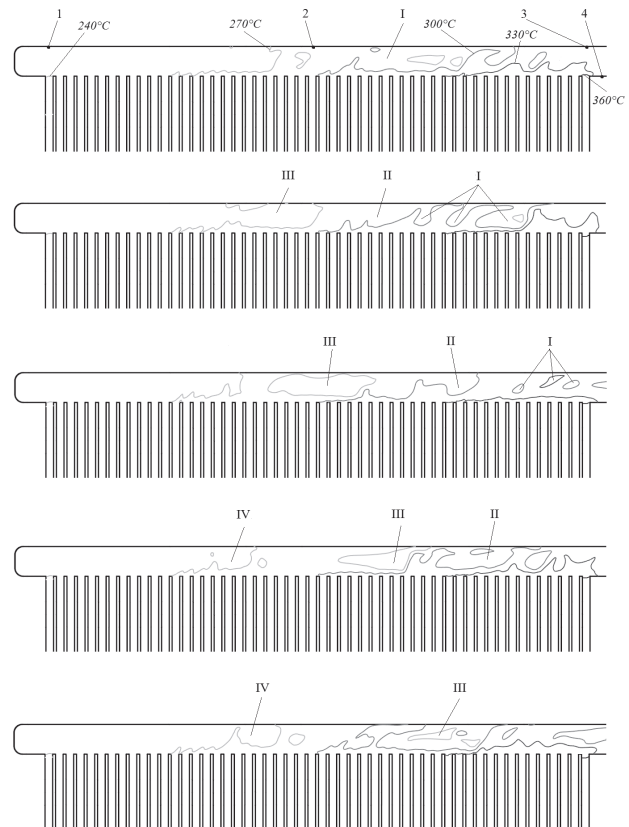


Figure 5. Sodium temperature in the AHX collecting header. Numbers I through IV show the ‘cold’ sodium volumes; 1–4 – test points; the italicized temperature values are for isothermal surfaces.

Analysis of the non-uniformity affecting factors

To analyze the factors that affect the non-uniformity of the AHX flow rate distribution, the FluidFlow code was used for calculating the header internal diameters of 200 mm and 300 mm with different diameters and equivalent lengths of the heat-exchange tubes. The equivalent tube length is the length of a straight tube, the hydraulic loss in which is equal to the total loss in the existing module tube. The calculation results are presented in Fig. 6 where d is the tube diameter, D is the header diameter, and L_{equ} is the equivalent tube length.

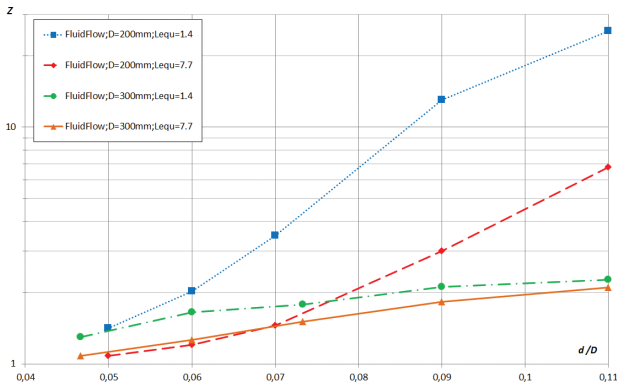


Figure 6. Non-uniformity of the sodium flow rate distribution by the AHX modules.

Increasing the outlet header diameter from 200 mm to 300 mm (all other geometrical characteristics of the tube bundle being equal) led to a 1.2 to 10 times smaller non-uniformity of the sodium distribution in the AHX. The non-uniformity of the sodium distribution in the AHX is the smaller, the smaller is L_{equ} (or the larger is the contribution of the hydraulic loss in the modules to the total hydraulic loss in the AHX). The smallest non-uniformity is achieved with a smaller diameter of the tubes, longer tubes and a larger diameter of the inlet header and the outlet header.

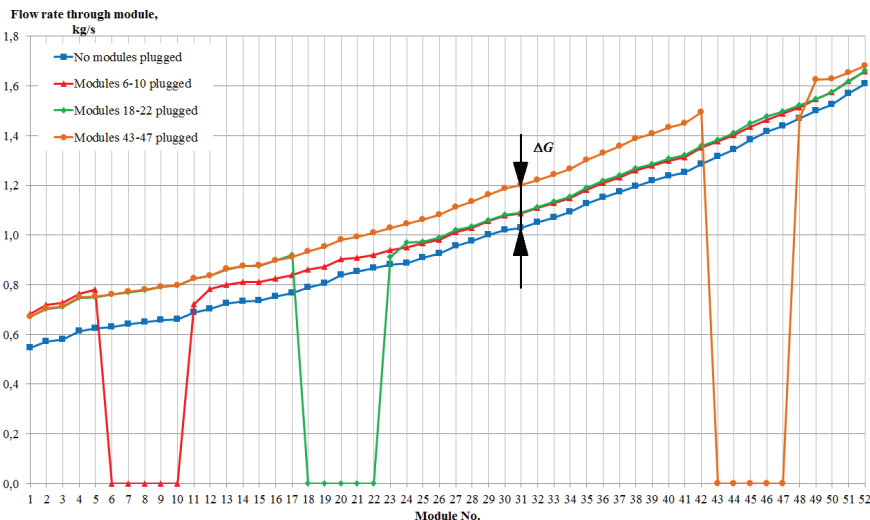


Figure 7. Sodium flow rate distribution by modules with different combinations of modules plugged.

Analysis of the tube plugging effect on the AHX header sodium flow rate and temperature distribution

There is a potentiality of the heat-exchange tube integrity loss and subsequent sodium leakage in the process of operation. For continued operation of the AHX, leaky modules can be plugged on the sodium side. To estimate the module plugging effect on the non-uniformity of the sodium flow rate distribution by modules and the mixing in the outlet header, a CFD analysis was undertaken for a number of options with the modules plugging at different AHX points. For all options, the total sodium flow rate through the AHX, and the sodium and air temperatures at the AHX inlet were assumed to be equal to rated values (see Table 1). The calculation results are presented in Table 3.

Table 3. Characteristics of the AHX calculated based on the FlowVision code (numerators) and the FluidFlow code (denominators)

Option	Number of plugged modules	Nos. of plugged modules	G_{min} , kg/s	G_{max} , kg/s	Z	A_t^* , °C
1	0	–	0.54 / 0.55	1.60 / 1.65	2.94 / 3.00	45
2	2	19-20	0.59 / 0.61	1.62 / 1.67	2.73 / 2.75	40
3	5	18–22	0.67 / 0.70	1.66 / 1.71	2.47 / 2.44	35
4	5	6–10	0.68 / 0.70	1.66 / 1.71	2.43 / 2.43	33
5	5	43–47	0.67 / 0.69	1.68 / 1.71	2.50 / 2.46	25
6	10	22–31	0.82 / 0.87	1.74 / 1.79	2.10 / 2.06	25

* A_t – maximum amplitude of the sodium temperature fluctuations at test point 3.

With some of the modules plugged, the total non-uniformity of the sodium flow rate distribution by the modules decreases due to an increased ratio of the hydraulic loss in the modules to the total hydraulic loss in the AHX, however, the plugging point does not have effect on the above non-uniformity and on the point at which the maximum amplitude of the sodium temperature fluctuations occurs (point 3).

To analyze this effect, the sodium flow rate distribution by the modules was calculated with five consecutive modules plugged in different AHX portions (Fig. 7).

The decrease in the non-uniformity with some of the modules being plugged is explained by the fact that the flow rate in the rest of the modules increases in a non-uniform manner. The increase in the flow rate, ΔG [kg/s], through the modules obeys the following dependences:

for modules upstream of the plugged group

$$\Delta G = (7n - 5) \times x^2 \times 10^{-6} + 0.0381n - 0.0525, \quad (3)$$

for modules downstream of the plugged group

$$\Delta G = (3n - 6) \times (52 - x)^2 \times 10^{-6} + 0.0191n - 0.048, \quad (4)$$

where n is the number of the consecutively installed modules plugged, and x is the module No.

The above relations are valid independent of the location of the group of the modules plugged. The accuracy of the calculations using formulas (3) and (4) is 20%, and the residual of the flow rate through the AHX does not exceed 5% with the total number of the modules plugged being not more than 20. The non-uniformity is smaller the larger is the number of the modules plugged and does not depend on the location of the group of such modules.

The maximum amplitude of fluctuations is observed in the region of the AHX header outlet. With the number of the modules plugged increased from 0 to 10, the difference in the sodium temperature between the initial module and the closing module decreases from 126 to 86 °C, and the amplitude of the temperature fluctuations decreases from 45 to 25 °C.

Conclusions

The non-uniformity of the sodium flow rate distribution by the AHX module tubes depends on the ratio of the

hydraulic loss in the tubes to the total loss in the module. The non-uniformity coefficient Z for the module is 1.04 calculated by the FlowVision three-dimensional code and 1.10 calculated by the FluidFlow one-dimensional code

The coefficient of non-uniformity Z by modules in the AHX is 2.94 calculated by the FlowVision code and 2.99 calculated by of the FluidFlow code, if the all modules in the AHX are working and the header diameter being 200 mm. The sodium temperature difference at the outlet of the extreme modules is 126 °C. The increase in the sodium temperature at the module outlet in the direction of the sodium flow leads to sodium not mixed in full in the AHX. The maximum amplitude of the sodium temperature fluctuations near the wall is 45 °C.

The non-uniformity of the sodium distribution by modules in the AHX depends on the ratio of the hydraulic loss in the modules to the total hydraulic loss in the AHX. If the header diameter increased to 300 mm, the non-uniformity coefficient by modules in the AHX decreases to 1.65, and there are practically no temperature fluctuations. While designing AHXs for advanced BN reactor facilities, it is recommended that the AHX inlet and outlet header diameter be increased to 300 mm for reducing the non-uniformity.

The coefficient of non-uniformity by modules in the AHX decreases when some of the modules are plugged. Approximations have been obtained which can be used to calculate the sodium flow rates through the modules upstream and downstream of the plugged group. With ten consecutive modules plugged, the maximum amplitude of the sodium temperature fluctuations near the wall decreases to 25 °C.

Sodium flow rate distribution in the AHX can be calculated using a one-dimensional code with the practically acceptable accuracy.

References

- Aksenov AA, Zhlukov SV, Osipov SL, Rogozhkin SA, Sazonova ML, Fadeev ID, Shepelev SF, Shmelev VV (2014) Development and verification of a turbulent heat transport model for sodium-based liquid metal coolants. *Vychislitel'naya Mekhanika Sploshnykh Sred* 7(3): 306–316. <https://doi.org/10.7242/1999-6691/2014.7.3.30> [in Russian]
- Cruickshank A, Judd AM (2005) Problems experienced during operation of the prototype fast reactor, Dounreay 1974–1994. *Proceeding of a technical committee meeting*. Reproduced by IAEA 2005: 51–79.
- FluidFlow (2021) User Guide. <https://support.fluidflowinfo.com> [accessed Oct. 24, 2021]
- Idelchik IYe (1992) *Handbook of Hydraulic Resistances*. Mashinostroyeniye Publ., Moscow, 672–672. [in Russian]
- Kimura N, Miyakoshi H, Kamide H (2007) Experimental investigation on transfer characteristics of temperature fluctuation from liquid sodium to wall in parallel triple-jet. *International Journal of Heat and Mass Transfer* 50: 2024–2036. <https://doi.org/10.1016/j.ijheat-masstransfer.2006.09.030>
- Knebel JU, Krebs L, Muller U, Axcell BP (1998) Experimental investigation of a confined heated sodium jet in a co-flow. *Journal of Fluid Mechanics* 368: 51–79. <https://doi.org/10.1017/S0022112098001463>
- Kolesnichenko IV, Khalilov RI, Shestakov AV, Krylov AN, Pakholkov VV, Pavlinov AM, Mamykin AD, Vasilyev AYU, Rogozhkin SA, Frik PG (2023) Mixing of different temperature flows of liquid sodium in the pipeline behind the tee. *Thermal Engineering* 70(3): 203–209. <https://doi.org/10.1134/S0040601523030023>
- Kolomiyets DO, Levchenko YuD, Sorokin AP (2014) An experimental study into the hydraulic resistance of the finned tube assembly in fast reactor air-cooled heat exchangers. *Izvestiya vuzov. Yadernaya Energetika* 1: 172–182. <https://doi.org/10.26583/npe.2014.1.13> [in Russian]
- Mochizuki H, Takano M (2009) Heat transfer in heat exchangers of sodium cooled fast reactors systems. *Nuclear Engineering and Design* 239: 295–307. <https://doi.org/10.1016/j.nucengdes.2008.10.013>